

# Ab initio investigation of competing instabilities in ferroelectric perovskite PbTiO<sub>3</sub>

Jacek C. Wojdel,<sup>1</sup> Patrick Hermet,<sup>2,3</sup> Mathias P. Ljungberg,<sup>1</sup> Philippe Ghosez,<sup>2</sup> and Jorge Íñiguez<sup>1</sup>

<sup>1</sup>*Institut de Ciència de Materials de Barcelona (ICMAB-CSIC), Campus UAB, E-08193 Bellaterra, Spain*

<sup>2</sup>*Physique Théorique des Matériaux, Université de Liège (B5), B-4000 Liège, Belgium*

<sup>3</sup>*Laboratoire Charles Coulomb (UMR CNRS 5221),  
Université Montpellier II, FR-34095 Montpellier Cédex 5, France*

We have developed first-principles models, based on a general parametrization of the full potential-energy surface, to investigate the lattice-dynamical properties of perovskite oxides. We discuss the application of our method to prototypic ferroelectric PbTiO<sub>3</sub>, showing that its properties are drastically affected by a competition between structural instabilities. Indeed, we confirm previous indications that the destructive interaction between the ferroelectric and antiferrodistortive (involving rotations of the O<sub>6</sub> octahedra) soft modes shifts PbTiO<sub>3</sub>'s Curie temperature by hundreds of degrees. Our theory provides unique insight into this gigantic effect and its dynamical character.

PACS numbers: 63.70.+h,64.60.De,77.80.B-,71.15.Mb

Perovskite oxides are a large family of materials of great fundamental and applied interest. In many cases, the structural and lattice-dynamical features of the compounds are critical to determine their properties. Most notably, this is the case of ferroelectric (FE) perovskites – whose spontaneous polarization is usually the result of a structural phase transition [1] – and related compounds such as magnetoelectric multiferroics – whose properties can be greatly enhanced by engineering the lattice response to external fields [2]. First-principles studies of lattice-dynamical phenomena are usually restricted to the limit of low temperatures, as the inclusion of thermal effects requires large simulation boxes (thousands of atoms to get a realistic description of most properties of interest) and a good sampling of configuration space (tens of thousands of Monte Carlo sweeps to compute statistical averages). Hence, it is not yet feasible to tackle such problems from first-principles directly.

The situation greatly improved with the development of effective models that (1) capture in a general and mathematically simple form the energy surface associated with the most relevant (i.e., lowest-energy) structural distortions and (2) whose parameters are computed from density-functional theory (DFT). This so-called *effective Hamiltonian* approach has been successfully applied to FE crystals like BaTiO<sub>3</sub> [3] and PbTiO<sub>3</sub> (PTO) [4], solid solutions like PbZr<sub>1-x</sub>Ti<sub>x</sub>O<sub>3</sub> (PZT) [5, 6], and even multiferroics like BiFeO<sub>3</sub> [7]. However, by neglecting all but the lowest-energy degrees of freedom, this scheme may introduce quantitative (e.g., in the description of thermal expansion [8]) and qualitative (e.g., whenever secondary modes are important [9]) errors. Further, the approach does not seem well suited to tackle structurally complex cases – from domain walls to heterostructures displaying interface-driven phenomena [10] – in which it may be difficult to identify a small set of distortions that capture the main effects. Shell models [11] and other schemes [12] providing a full atomistic description have also been derived from first-

principles for these materials; however, such approaches rely on specific forms of the interatomic potentials, which may restrict their accuracy and generality.

To overcome these limitations, we have developed an approach that provides a full atomistic description of the materials while retaining the general energy parametrization of the effective-Hamiltonian scheme. Here we describe our first application – to the study of PTO's FE phase transition –, which illustrates the predictive power and unique insights that the new method offers.

*Methods.*– Let us briefly describe our all-atom effective Hamiltonians, which will be presented in detail elsewhere [13]. As in the usual approach [3], we write the energy of the material as a Taylor series around a (cubic perovskite) reference structure. Our Taylor series, though, is a function of *all* the atomic degrees of freedom, not only the lowest-energy ones. It is convenient to split our variables into atomic displacements (generically denoted by  $u$ ) and global strains of the simulation box ( $\eta$ ), so that we can write the energy as

$$\begin{aligned} E(u, \eta) = & E_0 + E(u^2) + E(\eta^2) + E(\eta u^2) \\ & + E(u^3, u^4, \dots) + E(\eta^3, \eta^4, \dots) \\ & + E(\eta^2 u^2, \eta^3 u^2, \dots, \eta u^3, \dots). \end{aligned} \quad (1)$$

The first line in Eq. (1) contains the harmonic terms in  $u$  (i.e., the force-constant matrix  $\mathbf{K}$ ) and  $\eta$  (frozen-ion elastic tensor), which can be readily obtained from most first-principles codes; we computed them for PTO using density-functional perturbation theory as implemented in ABINIT [14–17]. Figure 1 shows the dispersion curves for the  $\kappa_{qs}$  eigenvalues of  $\mathbf{K}$ , which include a variety of structural instabilities of the cubic phase (i.e., distortions with  $\kappa_{qs} < 0$ ) and are exactly captured by our model [18]. The first line of Eq. (1) also includes the lowest-order non-zero  $\eta$ - $u$  couplings [19], which we obtain from the force-constant matrices computed for slightly strained cells. Such a *strain-phonon* coupling term is the only  $\eta$ - $u$  interaction considered in the usual effective Hamiltonians of

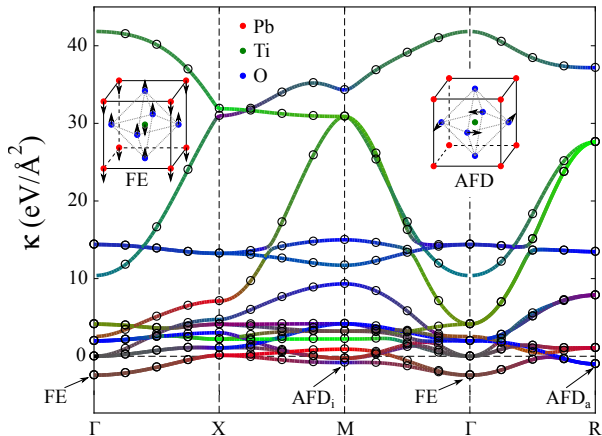


FIG. 1: (Color online.) Dispersion curves for the  $\kappa_{qs}$  eigenvalues of the force-constant matrix  $\mathbf{K}$  of PTO's cubic phase. Lines and circles are the results obtained *ab initio* and with our effective model, respectively. The line color indicates the atomic character of the eigenmode; red, green, and blue correspond to Pb, Ti, and O, respectively. Unstable ( $\kappa_{qs} < 0$ ) FE and AFD modes are sketched. The AFD<sub>a</sub> (AFD<sub>i</sub>) modes involve an antiphase (inphase) modulation of the O<sub>6</sub>-rotations along the rotation axis.

ferroelectrics.

The second and third lines of Eq. (1) include anharmonic interactions that in principle can extend to arbitrary order and need to be truncated [19]. We computed the parameters in such terms by fitting to the key features (energy, structure,  $\mathbf{K}$ -eigenmodes at selected  $\mathbf{q}$  points) of some relevant low-symmetry low-energy phases, which include several structures in which FE and antiferrodistortive (AFD) modes are condensed. [As described in Fig. 1, AFD modes may involve inphase (AFD<sub>i</sub>) and antiphase (AFD<sub>a</sub>) rotations of the O<sub>6</sub> octahedra; only the AFD<sub>a</sub> modes are relevant in the present discussion.] We first considered low-symmetry phases obtained by imposing the cubic cell ( $\eta = 0$ ) to compute the parameters in the  $E(u^3, u^4, \dots)$  term; we concluded it can be well approximated by (1) truncating the series at fourth order and (2) including only pairwise interactions between nearest-neighbor atoms (Pb-O and Ti-O). We then considered the fully-relaxed low-symmetry structures, and found that high-order  $\eta$ - $u$  couplings are needed in order to describe their main features accurately and, simultaneously, reproduce the first-order character of PTO's FE transition. (Our model includes selected  $\eta$ - $u$  couplings up to  $\eta^4 u^2$  order.) The  $E(\eta^3, \eta^4, \dots)$  term, on the other hand, could be neglected. The highest-order terms were chosen to be even powers of  $u$  and  $\eta$ , and the corresponding parameters restricted to be positive, to guarantee the global stability of the model.

Typically, the effective model of PTO used in this work reproduces the first-principles energies of the rel-

evant low-symmetry phases within a 15%, and their low-lying  $\mathbf{K}$ -eigenvalues within 0.5 eV/Å<sup>2</sup>. Note that our parameter-fitting procedure implicitly captures the usual features of atomistic models of ferroelectrics. For example, the double-well potential associated with the FE instability stems from (1) the unstable polar modes included at the harmonic level and (2) the anharmonic terms fitted to describe the stable low-symmetry phases obtained *ab initio*. The anharmonic interactions between modes are captured by fitting to the  $\kappa_{qs}$  spectrum of distorted structures, etc.

*Basic results.*— We solved our model by performing Monte Carlo simulations, typically using 20000 sweeps for thermalization and 80000 for computing averages at each considered temperature ( $T$ ). The simulation box contained  $8 \times 8 \times 8$  perovskite cells (i.e., 2560 atoms) and periodic boundary conditions were employed. ( $10 \times 10 \times 10$  supercells of 5000 atoms were used for  $T \approx T_C$ , where size effects become more relevant.) Figure 2 shows our basic results. Our model predicts that, at a temperature  $T_C \approx 325$  K, PTO undergoes a sharp transition between the high- $T$  cubic ( $Pm\bar{3}m$ ) and low- $T$  tetragonal ( $P4mm$ ) phases. This transition carries with it the deformation of the unit cell [Fig. 2(a)] and the development of an spontaneous polarization  $\mathbf{P}$  [Fig. 2(b)].

We confirmed that the polarization is the primary order parameter of the transformation by running simulations with the cubic cell fixed ( $\eta = 0$ ); in that case we still obtain a FE transition at a similar  $T_C$  [inset of Fig. 2(b)], but the polar phase has now a rhombohedral symmetry ( $R\bar{3}m$ ) with  $P_x = P_y = P_z$ . Further, at  $T \approx 200$  K we observe a second transition in which rotations of the O<sub>6</sub> octahedra around the polar axis are condensed (the symmetry is  $R\bar{3}c$  and the cell doubles). These results show the importance that the  $\eta$ - $u$  couplings have in determining PTO's behavior, and suggest that mechanical constraints (e.g., epitaxial strain) can greatly affect it.

Figure 2(c) shows the  $T$ -dependence of the atomic positions in PTO's unit cell. We find that, while the magnitude of the FE distortion depends strongly on  $T$ , the displacement pattern remains relatively constant. Hence, in this sense our results validate the usual assumption that the main features of the FE transition can be captured by effective models including only one type of polar distortion. Note also that at  $T \approx T_C$  the atomic displacements become *soft* [i.e., there is a large spread of their instantaneous values, as shown in the inset of Fig. 2(c)], which leads to an enhancement of the dielectric and (below  $T_C$ ) piezoelectric responses (not shown here).

Because it includes all the atoms, our model should correct the usual effective-Hamiltonian underestimation of the thermal expansion [8]. Indeed, above  $T_C$  we obtain an expansion coefficient  $\alpha = 18.2 \times 10^{-6} \text{ }^\circ\text{C}^{-1}$ , which exceeds the experimental value of  $12.6 \times 10^{-6} \text{ }^\circ\text{C}^{-1}$  [20].

*What controls  $T_C$ ?*— Our computed  $T_C$  is about 325 K, while the experimental result is around 760 K [20]. This

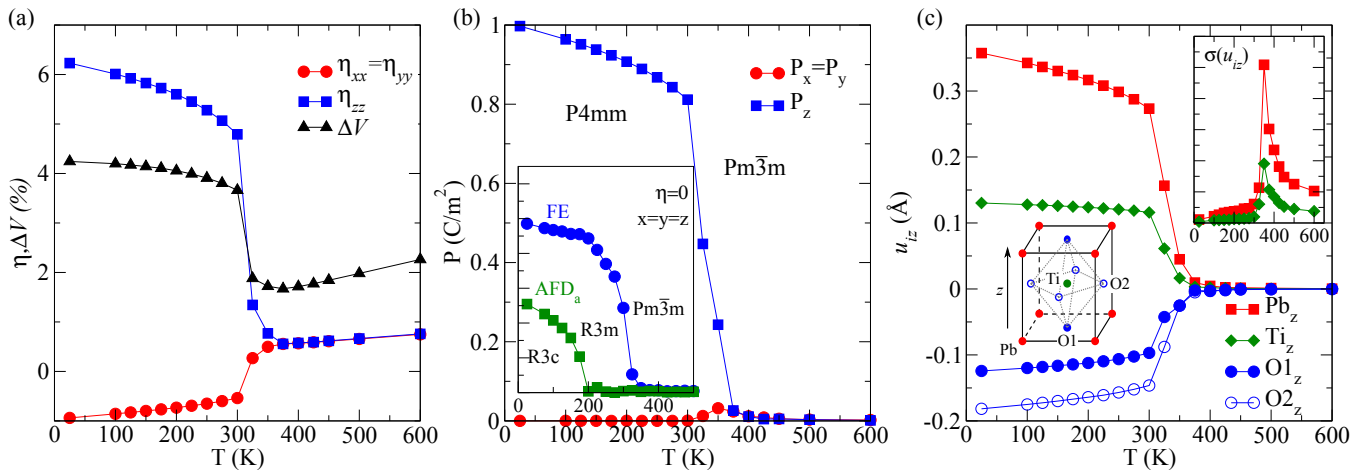


FIG. 2: (Color online.)  $T$ -dependence of the quantities characterizing PTO's FE transition. Panel (a): strains and volume change with respect to the reference cubic cell. Panel (b): Spontaneous polarization  $P_\alpha = v^{-1} \sum_{i\beta} Z_{i\beta,\alpha} u_{i\beta}$ , where  $v$  is the unit cell volume,  $\alpha$  and  $\beta$  are spatial directions,  $i$  labels atoms within the unit cell,  $Z_{i\beta,\alpha}$  are Born charges, and  $u_{i\beta}$  are supercell-averaged atomic displacements. Inset: results of simulations at fixed  $\eta = 0$ ; here, the FE and AFD<sub>a</sub> distortions are obtained by projecting the thermal-averaged configuration onto the corresponding unstable  $\mathbf{K}$ -eigenmodes of the cubic phase (see Fig. 1); units are arbitrary. Panel (c): Supercell-averaged displacements  $u_{i\alpha}$  along the direction of the spontaneous polarization. A global displacement is chosen so that  $\sum_i u_{i\alpha} = 0$ . Inset: standard deviation of the Pb and Ti displacements, in arbitrary units.

severe underestimation is surprising, as previous studies of PTO based on less-complete theories had shown a much better agreement with experiment. In particular, Waghmare and Rabe (WR) [4] constructed a model that neglects all degrees of freedom but the soft polar modes (treated as lattice Wannier functions) and cell strains, and obtained a value of 660 K [21].

We checked our model reproduces the energetics of the FE instabilities given by the WR Hamiltonian quite closely, despite the differences (e.g., DFT functionals, pseudopotentials) in the *ab initio* calculations employed to compute the parameters. Further, we ran simulations with modified versions of our model to test subtle features of the WR energy parametrization (e.g., the inclusion of high-order terms for the FE distortions), and concluded that they have a negligible effect on  $T_C$ .

We thus turned our attention to the qualitatively distinct features of our model. Most notably, we describe not only the FE instabilities, but also the unstable AFD distortions shown in Fig. 1. It is known that, in most perovskite oxides, the interaction between FE and AFD modes is a competitive one, so that they tend to suppress each other. The best studied case may be that of SrTiO<sub>3</sub> (STO), for which Zhong and Vanderbilt predicted, by means of an effective Hamiltonian approach, that the temperature of STO's AFD-related structural transition would be about 25% higher if the soft FE distortions of the material were suppressed [22].

The histograms in Fig. 3 show that similar effects occur in our PTO simulations. Above  $T_C$ , the AFD modes have relatively large amplitudes, comparable in

magnitude with those of the FE distortions. In contrast, they get significantly suppressed below  $T_C$ , in a way that clearly reflects the breaking of the cubic symmetry: the  $z$ -oriented spontaneous polarization restrains more strongly the transversal O<sub>6</sub>-rotational modes AFD<sub>ax</sub> and AFD<sub>ay</sub>. Note that the simultaneous occurrence of FE<sub>α</sub> and AFD<sub>αβ</sub> distortions, with  $\alpha \neq \beta$ , results in a significant deformation of the O<sub>6</sub> octahedra, which may explain why these transversal FE-AFD interactions are particularly destructive.

To investigate the effect of the AFD distortions on the FE transition temperature, we ran simulations in which the O<sub>6</sub> rotations were either totally (*no-AFD* case) or partly (*only-AFD<sub>z</sub>* case) suppressed. We imposed these constraints by restricting the motion of the oxygen atoms as shown in the sketches in Fig. 4. Let us stress that these constraints do not affect the energetics associated with the development of the spontaneous polarization, the FE ground state being exactly retained. (Even in the only-AFD<sub>z</sub> case – in which O<sub>6</sub> rotations are allowed only around the  $z$  axis, which breaks the cubic symmetry of the model –, we still keep the six equivalent FE minima with  $\mathbf{P}$  along the  $\pm x$ ,  $\pm y$ , and  $\pm z$  directions.) Figure 4 shows the results: In the no-AFD case we obtain  $T_C \approx 650$  K, which is very close to the WR result. We also ran this case at fixed  $\eta = 0$  (inset of Fig. 4) and obtained a similarly high  $T_C$ . In the only-AFD<sub>z</sub> case the calculated  $T_C$  is about 500 K, and the spontaneous polarization is found to point specifically along  $z$ . (We checked this by running several independent simulations starting from the  $u = \eta = 0$  configuration.) Note that these effects

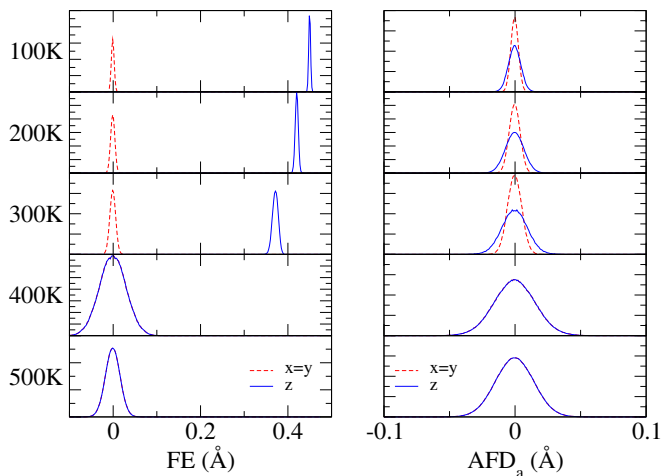


FIG. 3: (Color online.) Histograms of the FE and  $\text{AFD}_a$  distortions, which are quantified by projecting the instantaneous atomic structures on the corresponding unstable eigenmodes of the cubic reference phase.

– i.e., the shift in  $T_C$  and the preferential  $\mathbf{P}$ -direction in the only- $\text{AFD}_z$  case – have a strictly *dynamical* origin. For example, in our only- $\text{AFD}_z$  simulations, the  $\text{AFD}_{az}$  component fluctuates around its zero average value and hampers the development of the polarization, especially along the perpendicular directions  $x$  and  $y$ . Thus,  $P_z$  is *dynamically* favored and condenses at  $T_C$ .

A couple of additional points are worth making. (1) We find that strain does not play a big role in how the FE-AFD competition affects  $T_C$ , as our regular and fixed-cell simulations lead to very similar results in this regard. Note that, in principle, one could have expected otherwise: Because the FE and AFD instabilities tend to react differently to an external pressure [23, 25, 26], a FE distortion should imply cell deformations that, in turn, should suppress the AFD modes, and *viceversa*. However, our simulations suggest that such an effect is not very important, probably because at the temperatures at which the FE-AFD competition is relevant – i.e., in the range from 350 K to 650 K where the material would be FE in absence of AFD modes –, the correlations between atomic displacements and strains are relatively small.

(2) Our claim that a destructive FE-AFD interaction exists in the fixed-cell case may seem surprising, as a combined FE+AFD ground state occurs for  $\eta = 0$  [see inset of Fig. 2(b)]. However, note that competing instabilities may not fully suppress each other, and that is the case here. To make the argument more quantitative, let us note that the fixed-cell FE phase lies  $-59$  meV/f.u. below the cubic reference structure, while we get the AFD phase at  $-56$  meV/f.u. The combined FE+AFD structure has an energy of  $-62$  meV/f.u., far above the value of  $-115$  meV/f.u. (where  $115 = 59+56$ ) that one would expect if the FE and AFD modes did not interact at all [24]. It is thus clear that these two instabilities com-

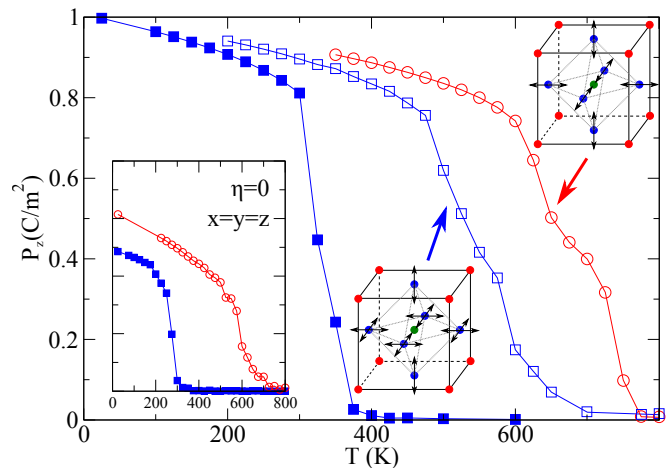


FIG. 4: (Color online.)  $T$ -dependence of the polarization (only one component is shown) as obtained in the regular (solid squares), only- $\text{AFD}_z$  (open squares), and no-AFD (open circles) cases. The arrows in the sketches indicate the oxygen displacements that are allowed in the only- $\text{AFD}_z$  and no-AFD cases; the motion of the Pb and Ti atoms is unconstrained. Inset: Results from simulations with fixed  $\eta = 0$ ; we show the spontaneous polarization distortion for the regular (filled squares) and no-AFD (open circles) cases.

pete in the fixed-cell case, even if they coexist at low temperatures. [In essence, in the regular case the polar distortion is larger ( $1.01$  C/m<sup>2</sup> at 0 K, as compared with  $0.57$  C/m<sup>2</sup> when  $\eta = 0$ ) and the FE-AFD interaction fully suppresses the AFD instability.]

Let us note that a very large competition-driven shift in  $T_C$  had already been predicted (but not much emphasized) for PZT by Kornev *et al.* [6]. The effective model used by these authors included some particular FE-AFD couplings that allowed them to rectify the very large  $T_C$  obtained previously from a simpler theory [5]. In contrast, our Hamiltonian captures the FE-AFD couplings in an implicit and non-specific way; in fact, when constructing our model we were not aware of the importance of this interaction, nor did we need to assume any form for it. Hence, our work ratifies that gigantic competition-driven effects can occur in PTO-related compounds. Interestingly, the analogous phenomena in  $\text{SrTiO}_3$ , which is generally considered the prototypic example for competing structural instabilities, are probably much smaller; in particular, Zhong and Vanderbilt obtained shifts in the transition temperatures of about 35 K [22].

The origin of the large difference between our computed  $T_C$  (325 K) and the experimental one (760 K) remains an open question. We ran additional tests to check the effect of some of the approximations made in our model [13], and did not observe any significant improvements. Hence, we tend to attribute the disagreement to the first-principles methods used to compute our Hamiltonian parameters. Indeed, to obtain the right  $T_C$ ,

the *ab initio* simulations should describe accurately (1) the strength of the FE instabilities, (2) the strength of the AFD instabilities, and (3) the magnitude of the FE-AFD coupling. Our results suggest that quantity (1) may be underestimated, and (2) and (3) overestimated, by our current calculations, despite our using the best DFT methods available for this task (i.e., recent functionals that have been shown to perform very well for these materials [27, 28]). Clearly,  $T_C$ 's large sensitivity to the FE-AFD competition sets a very stringent requirement for the accuracy of the *ab initio* calculations. Thus, our work suggests that, in spite of recent progress, we still lack DFT methods that describe accurately the thermodynamic properties of FE materials like PTO.

*Summary.*— We have introduced a novel approach for first-principles investigations of the lattice-dynamical properties of perovskite oxides. More precisely, we have developed effective models that are based on a general parametrization of the energy of the material (i.e., we make no *a priori* assumptions on the form of the interatomic couplings) and include all atomic degrees of freedom. The application of the new scheme to  $\text{PbTiO}_3$  has allowed us to investigate the competition of instabilities at play in this compound, which turns out to have dramatic effects in its properties. Indeed, we found that such a competition results in a reduction of  $\text{PbTiO}_3$ 's Curie temperature by as much as 300 K. Our simulations provide unique insights into this gigantic effect and its dynamical character.

Work supported by EC-FP7 project OxIDES (Grant No. CP-FP 228989-2). Also partly funded by MINECO-Spain (Grants No. MAT2010-18113, No. MAT2010-10093-E, and No. CSD2007-00041) and CSIC's JAE-doc program (JCW). Ph.G. thanks the Francqui Foundation for Research Professorship. We acknowledge discussions with L. Bellaiche, A. García, and P. García-Fernández.

---

[1] *Physics of ferroelectrics, A modern perspective*, K. Rabe, Ch.H. Ahn, and J.-M. Triscone, Eds. (Springer-Verlag Berlin Heidelberg 2007).

[2] J.C. Wojdeł and J. Íñiguez, Phys. Rev. Lett. **105**, 037208 (2010).

[3] W. Zhong, D. Vanderbilt, and K.M. Rabe, Phys. Rev. Lett. **73**, 1861 (1994); Phys. Rev. B **52**, 6301 (1995).

[4] U.V. Waghmare and K.M. Rabe, Phys. Rev. B **55**, 6161 (1997).

[5] L. Bellaiche, A. García, and D. Vanderbilt, Phys. Rev. Lett. **84**, 5427 (2000).

[6] I.A. Kornev, L. Bellaiche, P.-E. Janolin, B. Dkhil, and E. Suard, Phys. Rev. Lett. **97**, 157601 (2006).

[7] I.A. Kornev, S. Lisenkov, R. Haumont, B. Dkhil, and L. Bellaiche, Phys. Rev. Lett. **99**, 227602 (2007).

[8] S. Tinte, J. Íñiguez, K.M. Rabe, and D. Vanderbilt, Phys. Rev. B **67**, 064106 (2003).

[9] O. Diéguez, O.E. González-Vázquez, J.C. Wojdeł, and J. Íñiguez, Phys. Rev. B **83**, 094105 (2011).

[10] E. Bousquet, M. Dawber, N. Stucki, C. Lichtensteiger, P. Hermet, S. Gariglio, J.-M. Triscone, and P. Ghosez, Nature **452**, 732 (2008).

[11] M. Sepliarsky, A. Asthagiri, S.R. Phillpot, M.G. Stachiotti, and R.L. Migoni, Current Op. Sol. St. Mats. Sci. **9**, 107 (2005).

[12] Y.-H. Shin, V.R. Cooper, I. Grinberg, and A.M. Rappe, Phys. Rev. B **71**, 054104 (2005).

[13] J.C. Wojdeł, J. Íñiguez *et al.*, unpublished.

[14] All *ab initio* calculations were done with the ABINIT code [15], using the Wu-Cohen generalized gradient approximation to DFT [16]. The optimized pseudopotentials of Rappe *et al.* [17] were used to represent the ionic cores, treating the following electrons explicitly: Pb's  $6s^2$ ,  $6p^2$ , and  $5d^{10}$ ; Ti's  $3s^2$ ,  $3p^6$ ,  $3d^2$ , and  $4s^2$ ; and O's  $2s^2$  and  $2p^4$ . Electronic wave functions were represented in a plane-wave basis truncated at 1800 eV; we used a  $8 \times 8 \times 8$   $k$ -point grid to compute integrals in the Brillouin zone of the 5-atom perovskite cell, and equivalent meshes for other cells.

[15] X. Gonze *et al.*, Comp. Phys. Comm. **180**, 2582 (2009).

[16] Z. Wu and R.E. Cohen, Phys. Rev. B **73**, 235116 (2006).

[17] A.M. Rappe, K.M. Rabe, E. Kaxiras, and J.D. Joannopoulos, Phys. Rev. B **41**, 1227 (1990).

[18] At the harmonic level, we split the interatomic couplings into long-range and short-range components, following the standard procedure [P. Ghosez, E. Cockayne, U.V. Waghmare, and K.M. Rabe, Phys. Rev. B **60**, 836 (1999)]. This is the approach adopted for the usual effective Hamiltonians as well [3].

[19] Some terms are missing in Eq. (1) – e.g., those going as  $\eta u$  or  $\eta^2 u$  – because they are zero by symmetry for the cubic perovskite structure.

[20] M.J. Haun, E. Furman, S.J. Jang, H.A. McKinstry, and L.E. Cross, J. Appl. Phys. **62**, 3331 (1987).

[21] The  $T_C$  value that WR predicted for PTO is uncharacteristically close to experiment. For comparison, in the case of  $\text{BaTiO}_3$  the effective Hamiltonian of Zhong *et al.* [3] predicts a  $T_C$  (about 300 K) that is 25% smaller than the experimental result (about 400 K).

[22] W. Zhong and D. Vanderbilt, Phys. Rev. Lett. **74**, 2587 (1995).

[23] Moderate compression tends to suppress the usual FE distortion and favor  $O_6$  rotations. Such effects can be understood from steric arguments, and supporting evidence for specific materials can be found in the literature (e.g., for  $\text{PbTiO}_3$  [25, 26] and  $\text{SrTiO}_3$  [22]).

[24] For reference, the energy of the fully-relaxed tetragonal ground state is  $-123$  meV/f.u. in our model.

[25] P.-E. Janolin, P. Bouvier, J. Kreisel, P.A. Thomas, I.A. Kornev, L. Bellaiche, W. Crichton, M. Hanfland, and B. Dkhil, Phys. Rev. Lett. **101**, 237601 (2008).

[26] P. Ganesh and R.E. Cohen, J. Phys.: Condens. Matt. **21**, 064225 (2009).

[27] D.I. Bilc, R. Orlando, R. Shaltaf, G.-M. Rignanese, J. Íñiguez, and P. Ghosez, Phys. Rev. B **77**, 165107 (2008).

[28] R. Wahl, D. Vogtenhuber, and G. Kresse, Phys. Rev. B **78**, 104116 (2008).